

# THE EFFECT OF AXIAL COMPRESSION RATIO ON SEISMIC BEHAVIOR OF INFILLED REINFORCED CONCRETE FRAMES WITH PROFILED STEEL SHEET BRACING

FENG Ningning<sup>1</sup>, WU Changsheng<sup>2</sup>, MA Junyue<sup>1</sup>, MAO Xiaotian<sup>1</sup>

1. Changzhou Institute of Technology, Faculty of Civil Engineering, Civil Engineering & Architecture, Changzhou Jiangsu, No.666 Liaohe Road, China; fengningning1104@163.com
2. Southeast University, Institute of Geotechnical Engineering, Sipailou 2#, Nanjing Jiangsu, China; shengchangwu@126.com

## ABSTRACT

Seven infilled reinforced concrete (RC) frames strengthening with profiled steel sheet bracing are researched on the effect of axial compression ratio (0.3~0.9). Hysteretic curves, envelope curves, stiffness degradation curves, ductility and energy dissipation capacity are analysed in the finite element. The results show that profiled steel sheet bracing plays a good role in reinforcing infilled RC frames and the hysteretic curves express plump relatively. With the increase of axial compression ratio, the bearing capacity is improved significantly. The axial compression ratio has little effect on the lateral stiffness of the structure, and the initial stiffness increases slightly with the increase of axial compression ratio. The structure has good ductility when the axial compression ratio is less than 0.6. The ductility is declined with the increase of axial compression ratio. As the displacement increases, the energy dissipation capacity of the specimens increases. However, the energy dissipation capacity is reduced as the increase of axial compression ratio.

## KEYWORDS

Axial compression ratio, Profiled steel sheet bracing, RC frame, Seismic behaviour, Hysteretic curve

## INTRODUCTION

Steel bracing is the anti-lateral force member, which is used in reinforced concrete (RC) frame structures widely. Some scholars [1-4] have studied and proved the efficiency of steel bracing. The seismic performance of the structure has improved greatly. Tahamouli Roudsari et al. [5] adopted five different types including V-shaped, X-shaped, K-shaped, eccentrically braced and Y-shaped to reinforce RC frames. The damage characteristics and mechanical properties of RC frame were studied in the test. The experimental results showed that eccentrically braced had better ductility and less strength reduction factor than other braces. At the same time, X-shaped brace showed the good performance in improving the strength, stiffness and crack control in the process of strengthening. Guo and Fan [6] conducted dynamic characteristics and elastic seismic responses analysis on different reinforced concrete frames (5 floor, 8 floor and 12 floor) and RC frame with X-shaped central brace respectively. The results showed that X-shaped brace improved the lateral stiffness and reduced natural vibration period of the structure. In the action of horizontal earthquake, lateral displacement and storey drift angle were decreased. Yang et al. [7] based elastic analysis and elastic-plastic Pushover analysis on three RC frames, which had different

quantity of braces. The key research is the concept of RC frame with less steel brace. The research results indicated that collapse resistant capacity had enhanced with less steel brace. Fan et al. [8] studied eight layer framework strengthened with X-shaped brace. Pushover analysis was operated under the earthquake action. The research results showed that reasonable support increased the lateral stiffness of the structure effectively. At the same time, it decreased story drift and improved the seismic performance of the structure.

The above results show that steel braces can work with RC frame to obtain good seismic performance. On the basis of existing research, Cao and Feng [9] proposed RC frames strengthening with profiled steel sheet bracing which takes the influence of infill walls into consideration. Through the experimental study, the feasibility of infilled RC frame reinforcing with profiled steel sheet bracing had been verified. With the advantage of greater out-of-plane stiffness than ordinary plane, the profiled steel sheeting was adopted. The results showed that the strength is enhanced by 225%, the stiffness is increased by 108%, ductility is increased by 26.85%, cumulative energy is improved by 202.63%, respectively.

The seismic performances of multi-storey reinforced concrete frame structure reinforcing by profiled steel sheet bracing are different under different axial compression ratio. However, there are few studies on the seismic performance of infilled RC frame structures with axial compression ratio. Wang et al. [10] researched multi-storey and high-rise RC frame reinforcing by Y-shaped brace under different axial compression ratio. A nonlinear finite elements analysis was carried out to investigate the failure modes and the ultimate strength of structures. The results indicated that the bearing capacity and initial stiffness increased with the increase of axial compression ratio. Wang et al. [11] established square steel tube concrete frame model to analyse the influences of axial compression ratio. The results showed that the ductility of the frame decreased as the axial compression ratio increased.

Therefore, the objectives of this research was to reveal that the seismic performance of structures with different axial compression ratios and the influence on performance of structural reinforcement. On the basis of experimental study, finite element model of infilled RC frames with profiled steel sheet bracing are studied on the effect of different axial compression ratio. Structure seismic performances are investigated under axial compression ratio of frame column.

## Experimental model and finite element model

### Experimental model

The experimental model was completed in the structural engineering laboratory of Hohai University. Two-layer, one-span test specimen was carried under the low cyclic loading. Longitudinal bar and stirrup were HRB400. The diameter of longitudinal bar was 10 mm and the average yield strength was 382.11 MPa. The diameter of transversal tie was 8 mm and the average yield strength was 390.36 MPa. The average compressive strength of concrete was 38.23 MPa. The specimen design is shown in Figure 1. The steel type of profiled steel sheeting was Q235 and the model was YX35-250-1000. The thickness of profiled steel sheeting was 0.4 mm. The section of profiled steel sheeting is shown in Figure 2.

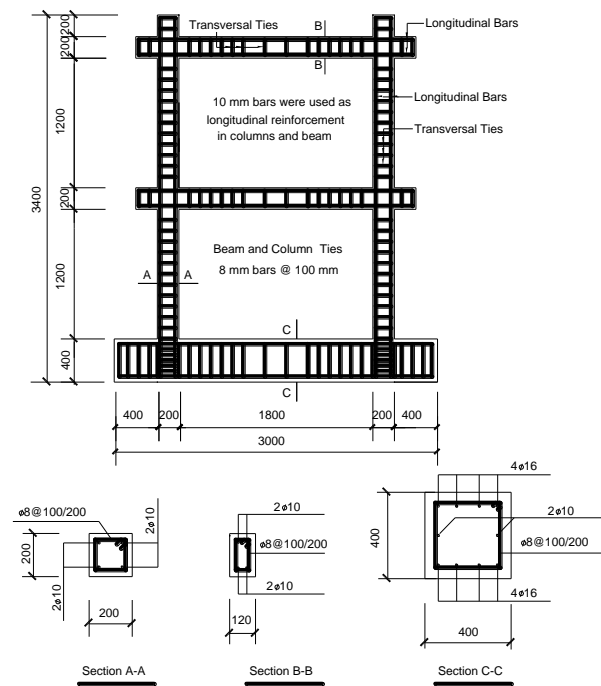


Fig. 1 – Specimen design

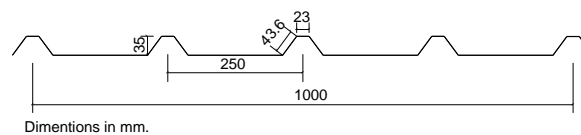


Fig. 2 – Sectional dimension of profiled steel sheet

### Finite element model

It was complicated when finite element models established the actual reinforced concrete structure. Hence, integral modelling was adopted in finite element modelling, which dispersed the longitudinal bar and stirrup into concrete. The software was adopted ANSYS and the unit of reinforced concrete used solid element SOLID 65. The reason was that the element can define concrete materials and three kinds of reinforcement materials. In other words, there were three kinds of reinforcement in different direction, and the selection of finite element model reinforcement was based on the Specimen design (Figure 1). According to the above material properties, the material constitutive model [12] was defined. The test model was arranged with infill walls inside RC frame. The two sides of infill walls were supported by profiled steel sheet bracing. The two faces were X-shaped and the test model is shown in Figure 3. It can be seen that test model was installed with steel plates and steel rods on beams and columns. And the channel steel was welded with steel plates inside RC frame. Infill walls were built in the channel steel, and tapping screws were used to connect profiled steel sheet bracing and channel steel. On the basis of test model, finite element modelling was simplified appropriately. The first simplification was that infill walls were equivalent to the diagonal pressure bar [12] (Figure 4 (a)). Simplification principle was basic on the main cracks of infill walls in the test developed along the diagonal line. The cracks were called as shear fracture. The test phenomenon accorded with equivalent diagonal brace model, which was proposed by Polyakov [13]. Polyakov showed that the infill walls in the frame were considered as a diagonal brace, which could bear pression but not tension; the second simplification was that profiled steel sheet bracing connected with RC frame directly. The common

nodes method was adopted to insure reliable connection. Namely, the common nodes method replaced steel plates and steel rods on beams and columns. Profiled steel sheet bracing was connected with beams and columns directly (Figure 4 (b)).

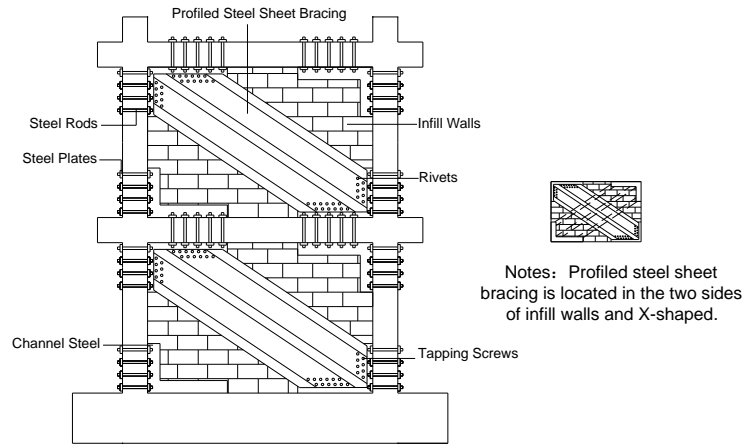


Fig. 3 – Test model

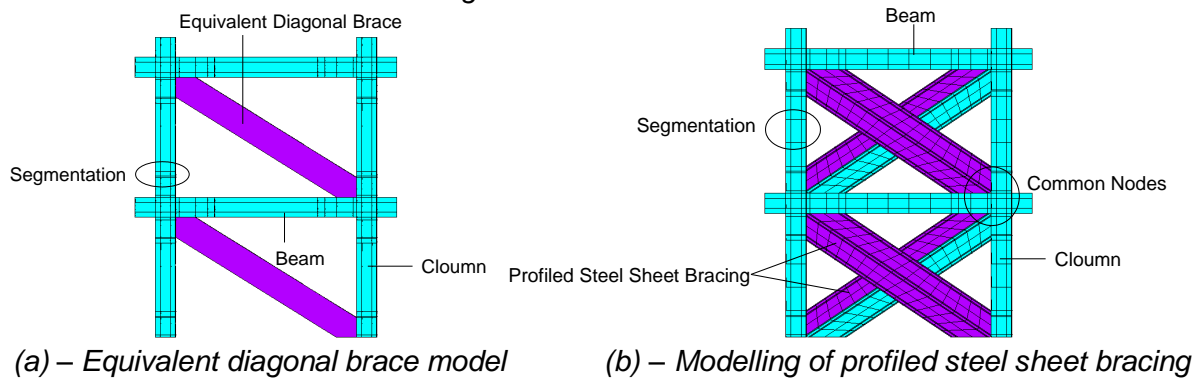


Fig.4 – Finite element model

### Validation of the finite element model

Hysteretic curves and skeleton curves in the test and finite element are shown in Figure 5. The experimental data came from the test [9] and the finite element analysis came from literature [12]. By comparing the two results, it can be seen that finite element analysis curve trend were similar with the test. It got gain access to the good plump curves. The maximum horizontal loads were 142.2 kN and 130.35 kN in the test and finite element and the deviation is 8.3 %. The compared results showed that effectiveness of profiled steel sheet bracing reinforcement. Profiled steel sheet bracing worked well with RC frame structure.

Because of the experimental conditions and fund assistance, it was impossible to pour more specimens in an experiment. However, axial compression ratio was an important factor affecting the seismic capacity of the frame. As a result, it was necessary to study axial compression ratio particularly. Based on the above research results, this paper focused on the research of seismic capacity of infilled walls RC frame with different axial compression ratio.

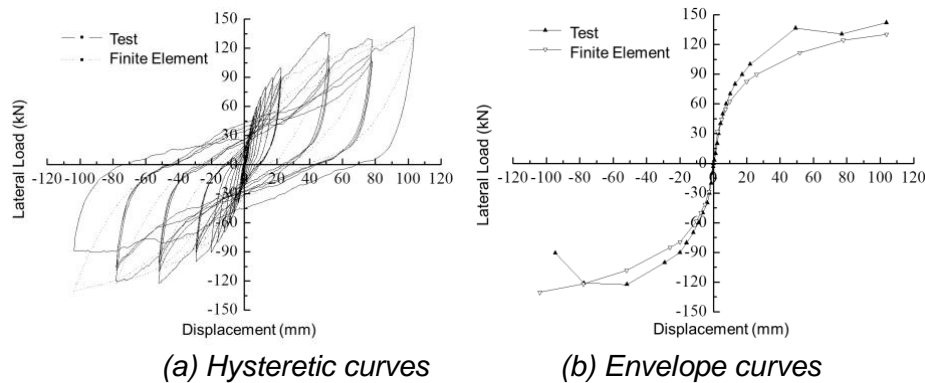


Fig.5 – Comparison of hysteretic curves and Envelope curves

### Selection of axial compression ratio

Axial compression ratio is one of the important factors in affecting the seismic capacity of frames. Enough ductility can be gained by limiting axial compression ratio of reinforced concrete frame structures in the earthquake. Structures or components can avoid brittle damage and meet the requirement of earthquake resistance as per Chinese Standard Design Code (2010). As a result, it is important to study the influence of different axial compression ratio on infilled RC frame structure. Controlling axial compression ratio is one of the important measures to ensure the necessary ductility of the structure. After Wenchuan Earthquake (China) in 2008, more attention is paid on structures with the design of axial compression ratio.

Axial compression ratio  $n$  is introduced as per Chinese Standard (2010), which can be expressed by axial pressure design value  $N$ , column section area  $A$  and concrete axial compressive strength design value  $f_c$ . The calculation can be expressed by Equation (1).

$$n = \frac{N}{f_c A} \tag{1}$$

In the test, the measured strength grade of concrete was C38 and corresponding design value of concrete axial compressive strength  $f_c$  is 18.1 N/mm<sup>2</sup> as per Chinese Standard (2010). Column cross-sectional area was denoted by  $A = 200 \times 200 = 40000 \text{ mm}^2$  and axial compression ratio was 0.27.

According to the axial compression ratio of common concrete column design, axial compression ratio is selected 0.3, 0.4, 0.5, 0.6, 0.7, 0.8 and 0.9. The values accord with the limit of axial compression ratio as per Chinese Standard (2010). The selected values are shown in Table 1.

Tab.1 - Axial compression ratio

Specimen	KJ1	KJ2	KJ3	KJ4	KJ5	KJ6	KJ7
Axial Pressure/kN	217.2	289.6	362	434.4	506.8	579.2	651.6
Axial Compression Ratio	0.3	0.4	0.5	0.6	0.7	0.8	0.9

### Hysteretic curves

Hysteretic curves of Specimens KJ1-KJ7 are shown in Figure 6. In the finite element analysis, the load steps were set up to control the incremental loading of the specimen. And finite element program realized the load steps. In order to facilitate analysis and comparison, different loads under the same displacement were selected for comparison. As can be seen from the figures, the residual deformation was very small and the horizontal load - displacement curves were close to the linear change. Specimens were in the initial stage of loading, which called elastic phase. There were small cracks in concrete with increasing lateral loads and horizontal displacements. The compression cracks could close and the structure deformation was small. The formed areas of

hysteresis loops by the addition and unloading were not big. After the displacement was loaded to 25.95 mm, the area of the hysteretic loops increased gradually. The frame entered into the elastic-plastic stage. Profiled steel sheet bracing supported the tensile force and the wall bear pressure. As a result, profiled steel sheet bracing and the wall worked together to improve the structural bearing capacity. Due to the concrete spalled and the compression zone of the column bottom destroyed, the hysteresis curves were difficult to simulate. Therefore, it considered that the test reached the limit state and the bearing capacity was the largest when the displacement reached to 103.8 mm. Finally, infilled RC frame structure strengthening by profiled steel sheet bracing gained plump hysteresis loop under the action of different axial compression ratio.

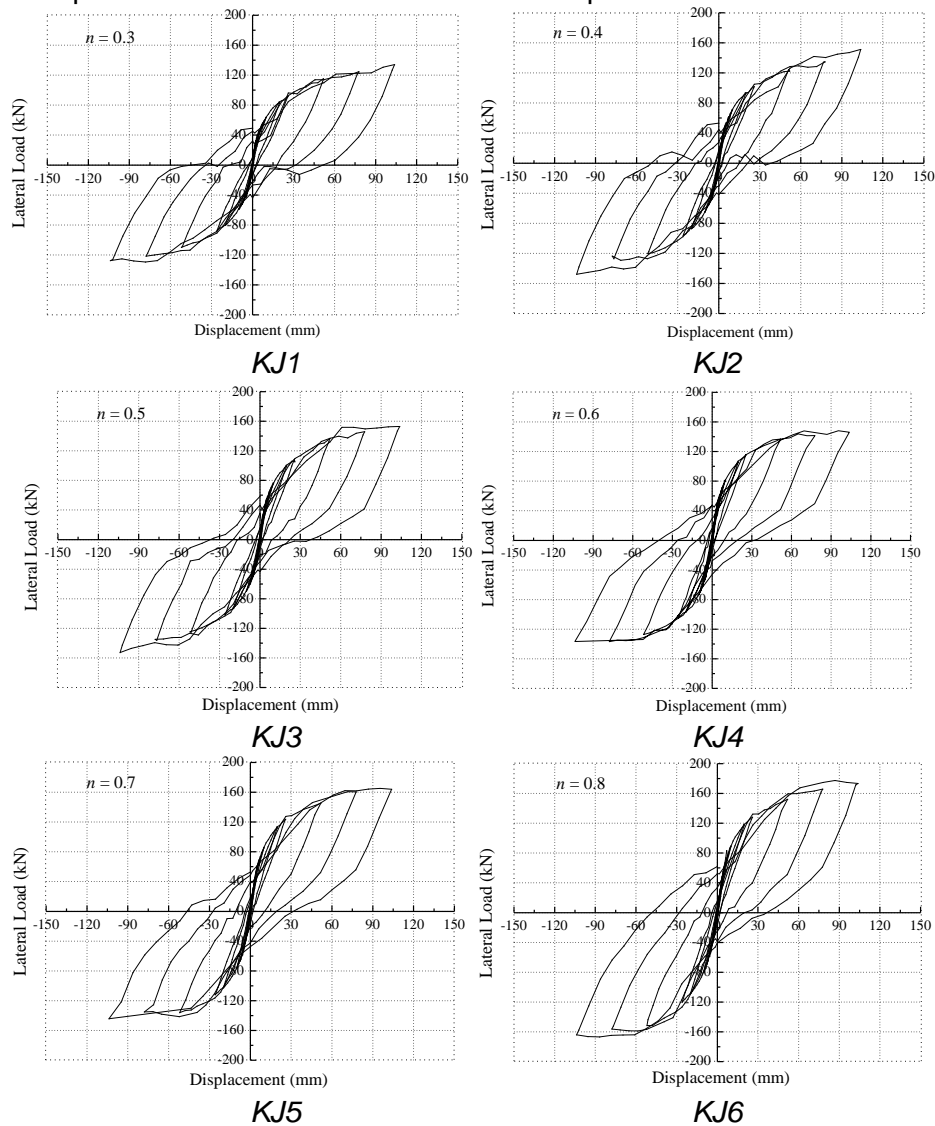
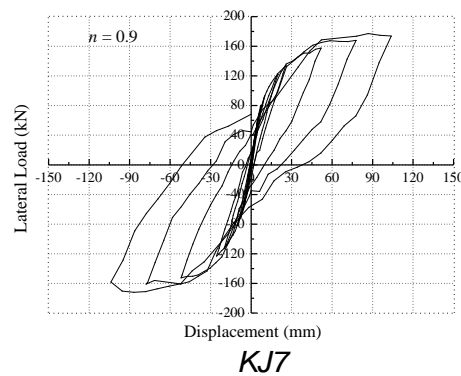


Fig.6 – Hysteretic curves





*Fig.6 – Hysteretic curves*

**Skeleton curves**

Skeleton curves of Specimens KJ1-KJ7 are shown in Figure 7. Load values at each stage are shown in Table 2. The skeleton curve reflected bearing force and deformation characteristics of the structure. It was an important basis for the study of the inelastic seismic response. The results showed that the maximum carrying capacity of Specimens KJ1, Specimens KJ2, Specimens KJ3 and Specimens KJ4 is 134.24 kN, 151.37 kN, 152.92 kN and 146.08 kN respectively. It can be seen from the results that Specimens KJ1 reached the minimum carrying capacity when the axial compression ratio was 0.3. The carrying capacity was similar when the axial compression ratio was 0.4 and 0.5. The bearing capacity of Specimens KJ3 is 1.02 % higher than that of Specimens KJ2. When the axial compression ratio reached 0.7, the maximum bearing capacity of the KJ5 was increased to 163.99kN. When the axial compression ratio was 0.8 and 0.9, the maximum bearing capacity of KJ6 and KJ7 were 173.34 kN and 173.99 kN respectively. With the increase of axial compression ratio, the bearing capacity increased when axial compression ratio was between 0.3 and 0.6 in the same displacement. When the axial compression ratio was 0.6, the bearing capacity decreased slightly. When the axial compression ratio was between 0.7 and 0.9, bearing capacity improved with the increase of axial compression ratio. And when axial compression ratio was 0.8 and 0.9, the bearing capacity was close relatively.

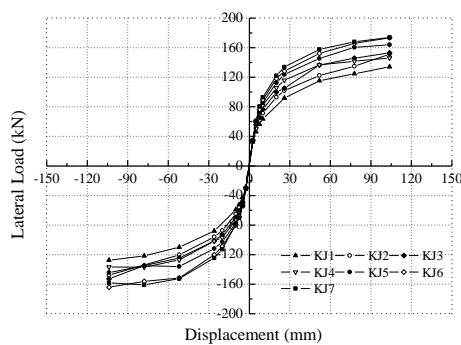


*Fig.7 – Envelope curves*

Tab.2 - Loads at each stage

Specimens	Cracking load /kN	Yield load /kN	The maximum load /kN
KJ1	32.75	85.76	134.24
KJ2	33.87	98.82	151.37
KJ3	34.42	102.02	152.92
KJ4	34.30	104.17	146.08
KJ5	34.44	117.01	163.99
KJ6	35.06	123.85	173.34
KJ7	35.89	127.09	173.99

### Rigidity degeneration

Rigidity degeneration curves of Specimens KJ1-KJ7 are shown in Figure 8. The initial and ultimate stiffness values are shown in Table 3. The secant stiffness [14] was adopted to describe stiffness degradation of specimens. At the initial stage of loading, concrete cracks developed quickly and stiffness degradation dropped fast. When the displacement reached 20 mm, the stiffness degradation rate slowed down. The initial stiffness of Specimens KJ1-KJ7 were 12.27 kN/mm, 12.71 kN/mm, 12.89 kN/mm, 12.93 kN/mm, 12.90 kN/mm, 12.93 kN/mm, 12.98 kN/mm, respectively. The ultimate stiffness of KJ1-KJ5 (axial compression ratio was 0.3-0.7) was 1.26 kN/mm-1.48 kN/mm. When axial compression ratio reached to 0.8-0.9, the ultimate stiffness of KJ6 and KJ7 reached 1.6 kN/mm.

With the increase of displacement, the rate of stiffness degradation of the Specimen KJ1-KJ7 approximated each other. Large axial compression ratio gained bigger initial stiffness. The reason was that the larger vertical load had stronger binding effect on the concrete, which improved the mechanical properties of the concrete and maintained the high lateral stiffness.

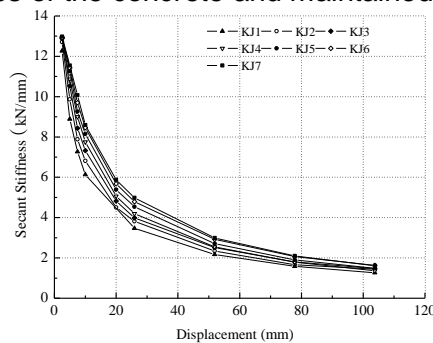


Fig.8 – Envelope curves

Tab.3 - Initial stiffness and ultimate stiffness

Specimens	KJ1	KJ2	KJ3	KJ4	KJ5	KJ6	KJ7
Initial stiffness/ (kN/mm)	12.27	12.71	12.89	12.93	12.90	12.93	12.98
Ultimate stiffness / (kN/mm)	1.26	1.44	1.47	1.36	1.48	1.63	1.61



### Ductility

Ductility curves of Specimens KJ1-KJ7 are shown in Figure 9. It can be seen that ductility factors [14] were 4.59, 4.32, 4.87, 5.31, 4.61, 4.41, 4.58 in the axial compression ratio 0.3-0.7. The ductility factor was all above 4.0. It indicated that profiled steel sheet bracing and infilled RC frame worked well together, which improved the ductility of the structure significantly. It can be seen from Figure 9, the ductility enhanced with the increase of axial compression ratio when axial compression ratio was between 0.4 and 0.6. However, the ductility decreased with the increase of axial compression ratio when axial compression ratio was greater than 0.6.

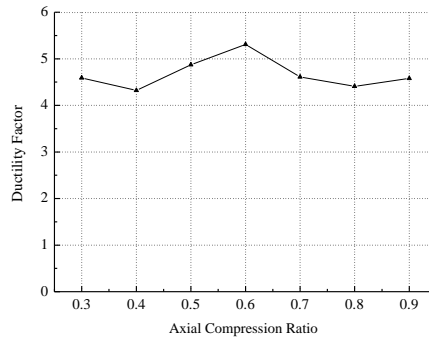


Fig.9 – Ductility curve

### Energy dissipation

Energy dissipation curves of Specimens KJ1-KJ7 are shown in Figure 10. It can be seen that the higher the value of equivalent viscous damping coefficient [14], the higher the ability of energy dissipating. In Figure 10, the equivalent viscous damping coefficient improved gradually with the increase of the displacement. The trend showed that the infilled RC frame structure strengthening with profiled steel sheet bracing obtained good energy dissipation capacity.

When the axial compression ratio was 0.3, the equivalent viscous damping coefficient gained a larger value. When the axial compression ratio is 0.4-0.9, the equivalent viscous damping coefficient decreased with the increase of axial compression ratio. It can be seen from that the lower axial compression ratio could get higher energy dissipation capacity. At the same time, the higher axial compression ratio decreased energy dissipating.

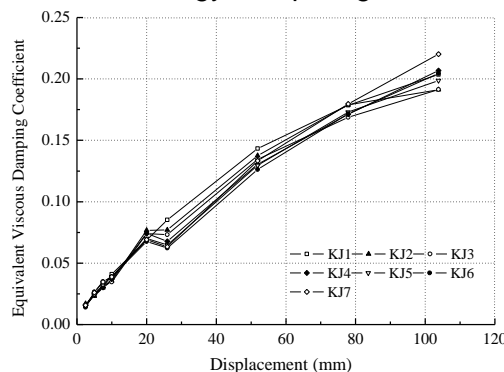


Fig.10 – Energy dissipation curve

### Conclusion

In this research, finite element models are verified by comparing with test results. Seven infilled RC frames strengthening with profiled steel sheet bracing specimens are studied in different axial compression ratio. The conclusions are as follows:

- (1) When the axial compression ratio was within the range of 0.3-0.6, the bearing capacity has been improved with the increase of axial compression ratio. The maximum bearing capacity range

was 134.24 kN-152.92 kN. Meanwhile, when the axial compression ratio was within the range of 0.7-0.9, the bearing capacity was enhanced with the increase of axial compression ratio. The maximum bearing capacity was 163.99 kN-173.99 kN. The maximum bearing capacity of the specimen was increased by 13.78 %-22.16 %. The infilled RC frame structure with high axial compression ratio was able to obtain higher seismic bearing capacity.

(2) The rate of stiffness degradation of seven specimens was almost the same under different axial compression ratio. When the axial compression ratio was 0.3-0.9, the initial stiffness value ranged from 12.27 kN/mm to 12.98 kN/mm and the ultimate stiffness ranged from 1.26 kN/mm to 1.61 kN/mm. With the increase of axial compression ratio, the initial stiffness and ultimate stiffness showed an increasing trend. However, the amplitude of increasing trend is not large. The effect of axial compression ratio on infilled RC frame structure was not significant.

(3) When the axial compression ratio was between 0.3 and 0.6, the ductility of infilled RC frame showed well. However, when the axial compression ratio was between 0.6 and 0.9, the ductility decreased. It showed that the smaller axial compression ratio, the better ductility of infilled RC frame. Excellent ductility can be achieved within the axial compression ratio of 0.6.

(4) The equivalent viscous damping coefficient and the energy dissipation capacity of Specimen KJ1-KJ7 were enhanced with the increase of displacement. It could get better energy dissipation capacity when the axial compression ratio was 0.3.

### Acknowledgment

The authors would like to acknowledge the Natural Science Foundation of the Jiangsu Higher Education Institutions of China (No: 18KJB560002), the Research Project of Ministry of Housing and Urban-Rural Development of Jiangsu province (No: 2017ZD233), Research Project of Changzhou institute of technology (No: YN1722), Student Research Training Program of Changzhou Institute of Technology (No: 2017079Z) and the National Program on Key Basic Research Project of China (973Program) (2015CB057803), which collectively funded this project.

### REFERENCES

- [1] ZHANG W. L., 2016. Seismic Behavior of RC Braced Frame Structures Research and Comparison Model Selection. PhD dissertation, Civil engineering, Lanzhou University of Technology, Lanzhou. (In China)
- [2] ZHAO B. C., WANG J. L., YU A. L., Gu Q., 2015. Design method of RC frame filled with Y-eccentrically steel brace. Journal of Xi'an university of architecture and technology (natural science edition), vol. 47(6): 799-803. (In China)
- [3] Maheri M. R., Akbari R., 2003. Seismic behaviour factor, R, for steel X-braced and knee-braced RC buildings. Engineering Structures, vol. 25(12): 1505-1513
- [4] Dubey S. K. D., Kute S. Y., 2013. Experimental investigation on the ultimate strength of partially infilled and steel-braced reinforced concrete frames. International Journal of Advanced Structural Engineering (IJASE), vol. 5(1): 1-10.
- [5] TahamouliRoudsaria M., Entezarib A., Hadidia M. H., Gandomian O., 2017. Experimental assessment of retrofitted RC frames with different steel braces. Structures, vol. 11(1): 206-217.
- [6] GUO J., FAN H. T., 2015. Seismic response properties of steel concentric X-centrally steel braced RC frames. Journal of Central South University (Science and Technology), vol. 46(6): 2299-2308. (In China)
- [7] YANG X., HE X. G., ZHAO Z. Z., QIAN J. R., 2015. The conception of RC frame structures with a few steel braces. Engineering Mechanics, vol. 32(S1): 129-135. (In China)
- [8] FAN H. T., WANG Z. X., ZHAO H. J., SUN A. F., 2013. Analysis of seismic performance of RC frame structure with X-bracings. Journal of Architecture and Civil Engineering, vol. (2): 35-41. (In China)
- [9] Cao P., Feng N., Wu K., 2014. Experimental study on infilled frames strengthened by profiled steel sheet bracing. Steel & Composite Structures, vol. 17(6): 777-790.

- [10] WANG J. L., ZHAO B. C., 2012. The effect of axial compression ratio on seismic property of Y-type eccentrically braced RC frames. *Journal of Suzhou University of Science and Technology (Engineering and Technology)*, vol. 25(4): 31-35. (In China)
- [11] WANG T. C., LU M. Q., 2005. The Finite element analysis of effect of axial load level on ductility of CFRT frames. *Journal of Jilin University (Engineering and Technology Edition)*, vol. 35(1): 70-75. (In China)
- [12] Feng N. N., CAO P. Z., QI Y. S., ZHAO F. H., 2017. Finite element analysis of infilled RC frames reinforced by profiled steel sheet bracing. *Steel Construction*, vol. 32(11): 37-41. (In China)
- [13] Polyakov, S. V., 1956. On the interactions between masonry filler walls and enclosing frame when loaded in the plane of the wall. *Translations in Earthquake Engineering Research Institute, Moscow, Russia.*
- [14] JGJ 101-2015, 2015. *Specification for seismic test of buildings.* China Architecture & Building Press, Beijing. (In China)